

Evaluation factors affecting landslide in Latyan catchment, Iran

Feiznia. S¹, Kouhpeima. A.², Moghadam Nia. A. L.³ and Ahmadi. H.⁴

²Young Researchers and Elite Club, Islamic Azad University, Karaj Branch, Karaj, Iran.

^{1,3,4}Faculty of Natural Resources, University of Tehran, Karaj, Iran.

ARTICLE INFO

Article history:

Received: 27 September 2016;

Received in revised form:

30 December 2016;

Accepted: 7 January 2017;

Keywords

Landslides,
Susceptibility,
Latyan,
Iran.

ABSTRACT

The main objective of this study is to evaluate the correlated factors of landslide using certainty factor (CF) Model in Latyan catchment, north Tehran, Iran. At first, a landslide inventory map was prepared using aerial photographs and the extensive field survey. For this purpose, 208 landslides were mapped and out of which 145 (70 %) were randomly selected for building landslide susceptibility models, while the remaining 63 (30 %) were used for validating the models. In this study, 10 conditioning factors with their classes were evaluated. These factors including: slope; slope aspect; altitude; plan curvature; lithology; land use; distance from faults, rivers and roads and topographic wetness index (TWI). The validation of landslide susceptibility map was carried out using receiver operating characteristic (ROC) curve. Results shows that the slope class 20°–30° (0.10640), slope aspect northwest (0.53335), the altitude 1800–2000 m (0.40805), curvature concave (0.00788), geology Jd (0.86675), Land Use forest (0.94588), distance from faults 6500–9500 m (0.47110), distance from river 0–200 m (0.25148) and distance from roads 0–500 m (0.24822) have the highest CF values. The result of ROC curve also shows that the certainty factor model has high value of AUC (0.832) which indicates the model employed in this study reasonably good accuracy in predicting the landslide susceptibility of Latyan catchment.

© 2017 Elixir All rights reserved.

Introduction

Among the various land degradation process, landslides are one of the most significant phenomena. The study of landslides has drawn worldwide attention mainly due to increasing awareness of its socio-economic impact as well as the increasing pressure of urbanization on the mountain environment (Aleotti and Chowdhury 1999). The impact of artificial structures and human interventions on mountain slopes followed by expansion of agricultural land and watershed management and overgrazing has compounded the landslide disaster problem in the country. To minimize the losses of human life and economic value, potential landslide-prone areas should, therefore, be identified. In this respect, landslide susceptibility assessment can provide valuable information essential for hazard mitigation through proper project planning and implementation. Landslide susceptibility is the likelihood of a landslide occurrence in an area on the basis of local terrain conditions (Brabb 1984). The advent of GIS has made the landslide susceptibility mapping easier these days (Jia et al. 2010; Karimi Nasab et al. 2010; Bednarik et al. 2012; Wang et al. 2011; Pradhan et al. 2011). Different methods to prepare landslide susceptibility and hazard maps using statistical methods and GIS tools were developed in the last decade (Van Westen et al. 2003; Guzzetti et al. 2005). The most common approaches proposed in the literature are bivariate (Saha et al. 2005; Pradhan et al. 2006; Magliulo et al. 2008; Pareek et al. 2010; Pradhan and Youssef 2010; Bednarik et al. 2010) and multivariate (Akguş et al. 2011; Pradhan 2010a; Oh et al. 2011; Choi et al. 2012). Other different methods have been proposed by several investigators, including weights-of-evidence methods (Regmi

et al. 2010a; Pourghasemi et al. 2012a, b), frequency ratio model (Pradhan et al. 2012), certainty factors (Pourghasemi et al. 2012a), information values (Saha et al. 2005). The aim of this paper is to produce landslide susceptibility map of Latyan catchment using certainty factor (CF) model. The model exploit information obtained from the inventory map to predict where landslides may occur in future.

The study area

The study area is located at the north of Tehran, Iran, one of the most landslide-prone areas in Iran. The watershed area lies between the longitudes of 51° 22' to 51° 51' N and latitudes of 35° 45' to 36° 05' E is mountainous and lies in the geological Alborz Folded zone (fig. 1). It covers four adjacent 1:50,000 topographic sheets and has an extent of about 70793 hectares. Latyan dam is located in the study area. Climate is cool mountainous based on Ambrose climatically classification. The mean annual rainfall is around 573 mm. In general, the precipitation falls between November and January based on the records from the Iranian Meteorological Department. Altitude in the study area varies between 1,500 to 4,325m. The parts of the study area are pasture and forest and the parts utilized for orchard and agricultural and residential.

Production of the thematic data layers

Various thematic data layers representing landslide conditioning factors namely slope, aspect, plan curvature, altitude, lithology, land use, distance from faults, distance from rivers, distance from roads, and topographic wetness index (TWI) were prepared. These factors fall under the category of preparatory factors, responsible for the occurrence of landslides in the region for which pertinent data can be collected from available resources as well as from the field.

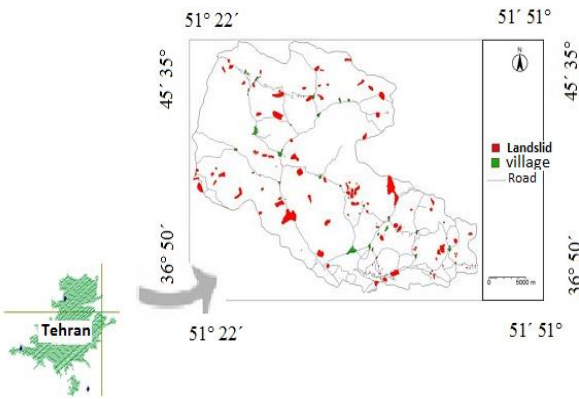


Fig 1. Location of the Latyan catchment and landslide inventory map.

Landslide inventory map

The mapping of existing landslides is essential to study the relationship between the landslide distribution and the conditioning factors. In order to produce a detailed and reliable landslide inventory map, extensive field surveys and observations are performed in the study area. A total of 208 landslides are identified and mapped by evaluating aerial photos in 1:25,000 scale with well supported by field surveys (Fig. 1). The mode of failure of the landslides identified in the study area are rotational and transitional sliding according to the landslide classification proposed by Varnes (1978). Of the 208 landslides identified, randomly 145 (70 %) locations were chosen for the landslide susceptibility maps, while the remaining 63 (30 %) cases were used for the model validation.

Slope

The main parameter of the slope stability analysis is the slope degree (Lee and Min 2001). Because the slope degree is directly related to the landslides, it is frequently used in preparing landslide susceptibility maps (Saha et al. 2005). For this reason, the slope map of the study area is prepared from the digital elevation model (DEM) and divided into nine slope categories (Fig. 2A). An integrated land and water information system (ILWIS3.3) software was used to discover in which slope group the landslide occurred and the rate of occurrence is observed.

Aspect

Aspect is accepted as a main landslide conditioning factor, and this parameter is considered in several studies (Lee et al. 2004a). In this study, the aspect map of the study area is produced to show the relationship between aspect and landslides (Fig. 2B). Aspects are grouped into 9 classes such as flat, north, northeast, east, southeast, south, southwest, west, and northwest.

Altitude

Altitude is also a relevant landslide conditioning factor used in this study. The altitude map was prepared from the 10 m * 10 m digital elevation model (Fig. 2C).

Distance from roads

Similar to the effect of the distance from rivers, landslides may occur on the road and on the side of slopes affected by roads. Change of slope (over steepening) due to excavation, additional load, change in hydrology, and drainage may affect the stress state and slope equilibrium.

In fact, during the field works, some landslides owing to road construction work are detected. For this reason, six different buffer zones are created on the path of the road to determine the effect of the road on the stability of slope (Fig.

2D). The landslide percentage distribution and its frequency ratio are determined considering the distance classes to the road by comparing the map of the distance to the road and the landslide inventory.

Distance from rivers

An important parameter that controls the stability of a slope is the saturation degree of the material on the slope. The closeness of the slope to drainage structures is another important factor in terms of stability. Streams may adversely affect stability by eroding the slopes or by saturating the lower part of material resulting in water level increases (Saha et al. 2005). For this reason, six different buffer zones were created within the study area to determine the degree to which the streams affected the slopes (Fig. 2E). Euclidean distance method was applied, and a visual inspection was done to see the correlation between the river and landslide.

Distance from faults

The distance from faults is calculated at 100-m intervals using the geological map (Fig. 2i). Euclidean distance method was applied, and a visual inspection was done to see the correlation between the faults and landslides. Faults form a line or zone of weakness characterized by heavily fractured rocks. Generally speaking, farther the distance from tectonic structures will result less numbers of landslides. Selective erosion and movement of water along fault planes promote such phenomena. A part from the major thrusts and faults derived from the geological maps, some complementary information regarding possible faults and structural dislocations was recognized as lineaments by means of image enhancement (filtering) of satellite imagery. The recognition of lineaments were performed step-by-step from large to smaller scales allowing the generalization of many neighboring small-order lineaments taking into account the spatial scale of the study (Fig. 2F).

Land use

Six different types of land use were described for this study using field surveys. These types of land use were pasture, forest, cultivation, Lake Dam, rocks, and residential areas (Fig. 2G). Most of the study area is covered by pasture. It is well known that land use and vegetation cover play important roles in the stability of slopes

Plan curvature

The term curvature is theoretically defined as the rate of change of slope gradient or aspect, usually in a particular direction. The curvature value can be evaluated by calculating the reciprocal value of the radius of curvature of that particular direction (Nefeslioglu et al. 2008b). Hence, while the curvature values of broad curves are small, the tight ones have higher values. Plan curvature is described as the curvature of a contour line formed by intersecting a horizontal plane with the surface (Fig. 2H). The influence of plan curvature on the slope erosion processes is the convergence or divergence of water during downhill flow (Oh and Pradhan 2011). For this reason, this parameter constitutes one of the conditioning factors controlling landslide occurrence (Nefeslioglu et al. 2008b). The plan curvature map was produced using a system for automated geoscientific analyses (SAGA) GIS.

Topographic wetness index (TWI)

Another topographic factor within the runoff model is the topographic wetness index (TWI).

A topographic wetness index measures the degree of accumulation of water at a site (Fig. 2I).

$$TWI = \ln(a/\tan b) \quad (1)$$

Where a is the cumulative upslope area draining through a point (per unit contour length) and $\tan b$ is the slope angle at the point. The $\ln(a/\tan b)$ index reflects the tendency of water to accumulate at any point in the catchment (in terms of a) and the tendency of gravitational forces to move that water down slope (expressed in terms of $\tan b$ as an approximate hydraulic gradient). The water infiltration primarily depends upon material properties such as permeability, pore water pressure, and effects on the soil strength.

Lithology

The landslide phenomenon, a part of geomorphologic studies, is related to the lithology of the land. Since different lithological units have different landslide susceptibility values, they are very important in providing data for susceptibility studies. For this reason, it is essential to group the lithological properties properly (Dai et al. 2001; Duman et al. 2006). Therefore, the geological map of the study area was prepared by Geological Survey of Iran (GSI) at 1:100,000 scale and was digitized in GIS. The study area is covered with various types of lithological units. The general geological setting of the area is shown in Fig. 2J.

Landslide susceptibility mapping

We used Certainty Factor (CF) model to obtain landslide susceptibility map. Certainty Factor (CF) is a model that has been applied by different researchers in landslide susceptibility mapping (Kanungo et al. 2011). The CF approach is one of the possible proposed favorability functions to handle the problem of combining different data layers and the heterogeneity and uncertainty of the input data. The certainty factors (CF) are given by the following equation:

$$CF = \begin{cases} \frac{ppa - pps}{ppa \times (1 - pps)} & \text{if } ppa > pps \\ \frac{pps - ppa}{pps \times (1 - pps)} & \text{if } ppa < pps \end{cases} \quad (2)$$

Where CF is the certainty factor, ppa is the area of landslide events occurring in class a / the area of class a and pps is the area of all landslide events in the study area / the area of catchment. The value of the certainty factor ranges between -1 and +1. The minimum -1 means definitely false and +1 means definitely true. A positive value means an increasing certainty in landslide occurrence, while a negative value corresponds to a decreasing certainty in landslide occurrence. A value close to 0 means that the prior probability is very similar to the conditional one; hence, it is difficult to give any indication about the certainty of the landslide occurrence. The CF values for all the condition factors were calculated by overlying landslides with the parameter class, that is, by calculating the landslide density and the CF values of all the layers using Eq. 2. Next, the CF values of the landslide conditioning factors were used for creating various CF layers (Table 1). Then, the calculated CF layers were combined pairwise. The combination of two CF values, X and Y, due to two different layers of information, is expressed as Z in Eq. 3, given below:

$$z = \begin{cases} x + y - xy, & x, y \geq 0 \\ \frac{x + y}{1 - \min(|x|, |y|)}, & x, y \text{ opposite sign} \\ x + y + xy, & x, y < 0 \end{cases} \quad (3)$$

The pairwise combination is performed repeatedly until all the CF layers are added to obtain the landslide susceptibility index (LSI). To make the results easier to interpret, the LSI values are grouped into susceptibility classes

to create landslide susceptibility zonation map for the study area. Several authors have applied various methods for dividing the LSI map. In this study, natural break classification method (Constantin et al. 2011; Xu et al. 2012) was used to divide the interval into five classes and a susceptibility map was prepared.

Results and discussion

The CF values of all landslide conditioning factors were determined using Eq. 2. The results of spatial relationship between landslide and conditioning factors using CF model are given in Table 1. The slope class $20^\circ - 30^\circ$ has the highest value of CF(0.10640) followed by $65^\circ - 100^\circ$ class (0.04911) and $30^\circ - 65^\circ$ class (0.03541) respectively. The lowest value of CF(-1) is for slope class 400–700. From this, it is clear that the landslide occurrence increases by the increase in slope percentage up to a certain extent, and then, it decreases. Few landslides occur on a very gentle slope and the landslide occurrence decreases as the slope becomes higher than 400° . In the case of slope aspect, the CF value is positive for east to northwest-facing slope facing, with the maximum value (0.53335) at northwest-facing slope followed by north-facing (0.49887) and northeast (0.22775) slopes respectively. The south-facing slopes are less prone to landslides as they have negative CF value. The CF values of altitude show that they are positive for the ranges of 1577–1800, 1800–2000, 2000–2300, and 2300–2500 with the highest value (0.40805) for the altitude ranging between 1800 and 2000 m. The CF value decreases with both the increase and decrease in altitude. It becomes negative after 2500 m. This shows that the probability of landslide occurrence decreases as the altitude becomes higher than 2500 m. In the case of curvature, the CF value is positive (0.00788) only on concave and flat slopes. The convex slopes are not responsible for landslide hazard in this area. For the geology, it can be seen that the Jd (CF = 0.86675), E2ts (CF = 0.85045), QI (CF = 0.81498), Pd (CF = 0.80082), JI (CF = 0.79548), T1 (CF = 0.71299), ϵ bt (CF = 0.55083), Qf (CF = 0.51018), M (CF = 0.42713), Eksh (CF = 0.42178), Efs1 (CF = 0.38818), Ekt (CF = 0.34381), and Qs (CF = 0.10809) are found to be more susceptible to sliding respectively (Table 1). In the case of land use, positive value of CF is seen on agricultural lands, forest lands, pasture lands and Lake Dam, while negative value of CF is seen on residential and rocks. In this case the forest lands is the highest susceptibility to landslide (CF= 0.94588) and then Lake Dam (CF=34137) is second. The high susceptibility of these two sources may be due to the human activities in the forest and the area around Lake Dam. In the case of distance from faults, the intervals 4000–6500, 6500–9500 m have weights (CF) of 0.34713 and 0.47110, respectively. Other intervals have negative CF. The influence of drainage system upon the landslide susceptibility was also analyzed by identifying the drainage river line by buffering. The distance range of 0–200 m (0.25148) has the highest CF value, followed order by 200–400 m (0.16184) and 400–650 m (0.03383).

This indicates that the landslide occurrence decreases with the increase in distance from the river. In the case of distance from roads, the intervals 0–500 (0.24822) has higher CF values, that is, the landslide susceptibility is higher in these ranges. The relation between TWI landslide probabilities showed that 12.63–24.70 class has the highest value of CF (0.17166).

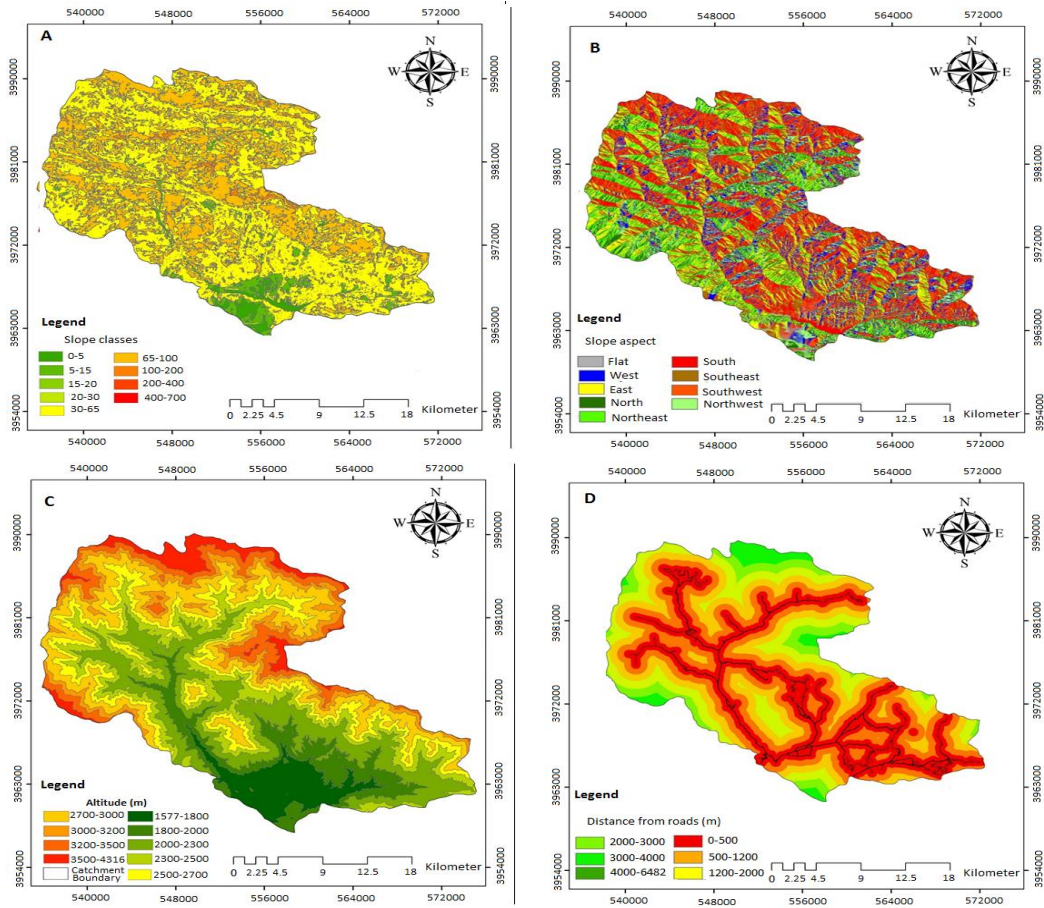


Fig 2. Thematic maps used in this study. A Slope map (%); B Aspect map; C Elevation map (m); D Distance from road map (m); E Distance from river map (m); F Distance from fault map (m); G Land use map; H Plan curvature map; I Topographic wetness index map; J Lithology map.

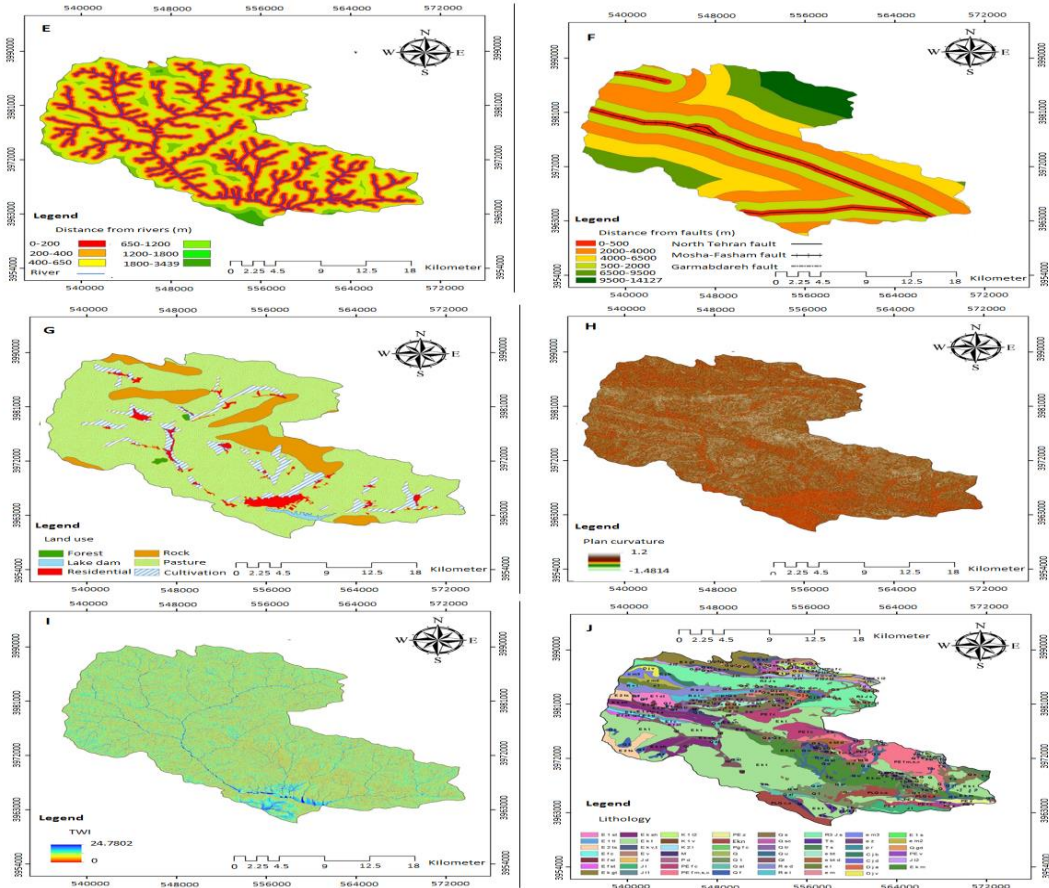


Table 1. Spatial relationship between each landslide conditioning factor and landslide by certainty factor.

| Factor | Class | Landslide area | Class area | PPa | PPs | CF |
|--------------------------|-------------------------|----------------|------------|-----------|---------|----------|
| Slope degree (%) | 0-5 | 77.362 | 1529.478 | 0.05058 | 0.05895 | -0.14960 |
| | 5-15 | 91.904 | 3050.289 | 0.03013 | 0.05895 | -0.50412 |
| | 15-20 | 21.333 | 541.817 | 0.03937 | 0.05895 | -0.34576 |
| | 20-30 | 68.255 | 1041.832 | 0.06551 | 0.05895 | 0.10640 |
| | 30-65 | 2398.300 | 39324.918 | 0.06099 | 0.05895 | 0.03541 |
| | 65-100 | 1481.079 | 23961.443 | 0.06181 | 0.05895 | 0.04911 |
| | 100-200 | 28.428 | 1157.413 | 0.02456 | 0.05895 | -0.59807 |
| | 200-400 | 0.144 | 3.583 | 0.04021 | 0.05895 | -0.33119 |
| | 400-700 | 0.000 | 0.146 | 0.000 | 0.05895 | -1 |
| | Slope aspect | Flat | 18.676 | 631.330 | 0.02958 | 0.05895 |
| North | | 254.657 | 2291.711 | 0.11112 | 0.05895 | 0.49887 |
| Northeast | | 709.638 | 9457.207 | 0.07504 | 0.05895 | 0.22775 |
| Northwest | | 1011.998 | 8550.096 | 0.11836 | 0.05895 | 0.53335 |
| South | | 411.447 | 12239.897 | 0.03362 | 0.05895 | -0.44476 |
| Southeast | | 404.328 | 9497.201 | 0.04257 | 0.05895 | -0.29022 |
| Southwest | | 420.847 | 12153.502 | 0.03463 | 0.05895 | -0.42744 |
| East | | 493.222 | 7959.547 | 0.06197 | 0.05895 | 0.05164 |
| West | | 441.985 | 7830.522 | 0.05644 | 0.05895 | -0.04513 |
| Altitude (m) | | 1577-1800 | 403.053 | 5145.383 | 0.07833 | 0.05895 |
| | 1800-2000 | 626.360 | 6544.745 | 0.09570 | 0.05895 | 0.40805 |
| | 2000-2300 | 984.919 | 12967.374 | 0.07595 | 0.05895 | 0.23783 |
| | 2300-2500 | 684.733 | 9719.352 | 0.07045 | 0.05895 | 0.17340 |
| | 2500-2700 | 436.028 | 9365.858 | 0.04656 | 0.05895 | -0.22059 |
| | 2700-3000 | 586.329 | 12390.143 | 0.04732 | 0.05895 | -0.20711 |
| | 3000-3200 | 164.076 | 5895.209 | 0.02783 | 0.05895 | -0.54302 |
| | 3200-3500 | 186.979 | 5396.221 | 0.03465 | 0.05895 | -0.42706 |
| | 3500-4316 | 100.902 | 3368.044 | 0.02996 | 0.05895 | -0.50702 |
| | Distance from roads (m) | 0-500 | 1531.085 | 19904.260 | 0.07692 | 0.05895 |
| 500-1200 | | 1114.242 | 18934.538 | 0.05885 | 0.05895 | -0.00194 |
| 1200-2000 | | 781.327 | 14666.862 | 0.05327 | 0.05895 | -0.10182 |
| 2000-3000 | | 509.086 | 10493.617 | 0.04851 | 0.05895 | -0.18613 |
| 3000-4000 | | 193.072 | 4416.998 | 0.04371 | 0.05895 | -0.27038 |
| 4000-6483 | | 44.547 | 2376.040 | 0.01875 | 0.05895 | -0.69502 |
| Distance from rivers (m) | 0-200 | 1330.233 | 17223.856 | 0.07723 | 0.05895 | 0.25148 |
| | 200-400 | 1013.387 | 14571.316 | 0.06955 | 0.05895 | 0.16184 |
| | 400-650 | 921.513 | 15133.258 | 0.06089 | 0.05895 | 0.03383 |
| | 650-1200 | 748.935 | 19812.514 | 0.03780 | 0.05895 | -0.37291 |
| Distance from faults (m) | 0-500 | 284.316 | 6665.174 | 0.04266 | 0.05895 | -0.28876 |
| | 500-2000 | 844.068 | 17967.967 | 0.04698 | 0.05895 | -0.21319 |
| | 2000-4000 | 828.255 | 20010.364 | 0.04139 | 0.05895 | -0.31077 |
| | 4000-6500 | 1203.165 | 13741.669 | 0.08756 | 0.05895 | 0.34713 |
| | 6500-9500 | 866.193 | 8178.981 | 0.10590 | 0.05895 | 0.47110 |
| | > 9500 | 147.421 | 4228.704 | 0.03486 | 0.05895 | -0.42342 |
| Land use | Residential | 96.007 | 2277.587 | 0.04215 | 0.05895 | -0.29754 |
| | Forest | 90.139 | 168.013 | 0.53650 | 0.05895 | 0.94588 |
| | Agriculture | 410.223 | 5835.933 | 0.07029 | 0.05895 | 0.17140 |
| | Pasture | 3263.313 | 53914.370 | 0.06053 | 0.05895 | 0.02762 |
| | Rock | 284.797 | 8261.940 | 0.03447 | 0.05895 | -0.43012 |
| | Lake dam | 29.089 | 334.909 | 0.08686 | 0.05895 | 0.34137 |
| Plan curvature | -1.48 - -0.001 | 1469.671 | 24744.026 | 0.05939 | 0.05895 | 0.00788 |
| | -0.001 - 0.001 | 1136.738 | 18735.857 | 0.06067 | 0.05895 | -0.03008 |
| | 0.001 - 1.2 | 1566.541 | 27310.815 | 0.05736 | 0.05895 | -0.02870 |
| TWI | 0 - 7.67 | 1650.470 | 28601.820 | 0.05771 | 0.05895 | -0.02249 |
| | 7.67 - 12.63 | 1877.678 | 33107.100 | 0.05672 | 0.05895 | -0.04027 |
| | 12.63 - 24.7 | 638.709 | 9083.820 | 0.07031 | 0.05895 | 0.17166 |
| Lithology | C j b | 18.66 | 739.128 | 0.02525 | 0.05895 | -0.58655 |
| | C j d | 2.13 | 172.008 | 0.01238 | 0.05895 | -0.79985 |
| | D j a | 0.00 | 287.556 | 0 | 0.05895 | -1 |
| | D j v | 0.00 | 252.628 | 0 | 0.05895 | -1 |
| | E 1 s | 0.00 | 130.872 | 0 | 0.05895 | -1 |
| | E 1 st | 57.41 | 1128.840 | 0.05086 | 0.05895 | -0.14471 |
| | E 1 tl | 0.00 | 247.682 | 0 | 0.05895 | -1 |
| | E 2 ts | 356.49 | 1207.490 | 0.29523 | 0.05895 | 0.85045 |

| | | | | | | |
|--|-----------|---------|-----------|---------|---------|----------|
| | É bt | 48.15 | 393.386 | 0.12240 | 0.05895 | 0.55083 |
| | É bt d | 17.00 | 579.575 | 0.02933 | 0.05895 | -0.51762 |
| | E f c | 0.00 | 239.535 | 0 | 0.05895 | -1 |
| | E f sl | 26.47 | 284.966 | 0.09289 | 0.05895 | 0.38818 |
| | E f st | 0.00 | 248.861 | 0 | 0.05895 | -1 |
| | E k gt | 0.00 | 1918.650 | 0 | 0.05895 | -1 |
| | E k m | 102.13 | 4571.230 | 0.02234 | 0.05895 | -0.63523 |
| | E k sh | 269.50 | 2756.900 | 0.09776 | 0.05895 | 0.42178 |
| | E k t | 1617.34 | 18557.900 | 0.08715 | 0.05895 | 0.34381 |
| | E k v,t | 0.00 | 646.552 | 0 | 0.05895 | -1 |
| | É l | 19.04 | 1162.390 | 0.01638 | 0.05895 | -0.73422 |
| | É m | 0.00 | 304.011 | 0 | 0.05895 | -1 |
| | É m2 | 0.00 | 419.260 | 0 | 0.05895 | -1 |
| | É m3 | 0.00 | 556.677 | 0 | 0.05895 | -1 |
| | E v | 0.00 | 218.665 | 0 | 0.05895 | -1 |
| | É z | 11.90 | 606.503 | 0.01962 | 0.05895 | -0.68053 |
| | J d | 10.67 | 33.354 | 0.31979 | 0.05895 | 0.86675 |
| | J l | 232.53 | 991.645 | 0.23449 | 0.05895 | 0.79548 |
| | J l1 | 0.00 | 316.697 | 0 | 0.05895 | -1 |
| | J l2 | 0.00 | 775.642 | 0 | 0.05895 | -1 |
| | K 1 l2 | 0.00 | 357.048 | 0 | 0.05895 | -1 |
| | K 1 v | 0.00 | 379.318 | 0 | 0.05895 | -1 |
| | K 2 l | 0.00 | 275.579 | 0 | 0.05895 | -1 |
| | M | 77.98 | 791.021 | 0.09858 | 0.05895 | 0.42713 |
| | P d | 9.15 | 38.238 | 0.23927 | 0.05895 | 0.80082 |
| | p r | 0.00 | 69.744 | 0 | 0.05895 | -1 |
| | PE fc | 87.40 | 3040.440 | 0.02874 | 0.05895 | -0.52759 |
| | PE fm,s,c | 133.28 | 3216.220 | 0.04144 | 0.05895 | -0.30995 |
| | PE v | 0.00 | 131.642 | 0 | 0.05895 | -1 |
| | PE z | 29.03 | 558.973 | 0.05194 | 0.05895 | -0.12548 |
| | Pg f c | 0.00 | 37.735 | 0 | 0.05895 | -1 |
| | Ekn | 44.61 | 2436.700 | 0.01831 | 0.05895 | -0.70231 |
| | Q | 0.00 | 353.083 | 0 | 0.05895 | -1 |
| | Q l | 86.90 | 2008.330 | 0.04327 | 0.05895 | -0.27812 |
| | Q al | 48.20 | 902.943 | 0.05338 | 0.05895 | -0.09985 |
| | Q f | 62.17 | 548.267 | 0.11340 | 0.05895 | 0.51018 |
| | Q gd | 0.000 | 85.895 | 0 | 0.05895 | -1 |
| | Q s | 208.699 | 3179.910 | 0.06563 | 0.05895 | 0.10809 |
| | Q sc | 0.000 | 521.096 | 0 | 0.05895 | -1 |
| | Q tr | 6.101 | 183.324 | 0.03328 | 0.05895 | -0.45046 |
| | Q u | 45.851 | 1559.260 | 0.02941 | 0.05895 | -0.51641 |
| | Ql | 224.213 | 886.400 | 0.25295 | 0.05895 | 0.81498 |
| | R e d | 66.300 | 1342.870 | 0.04937 | 0.05895 | -0.17099 |
| | R e l | 20.945 | 728.803 | 0.02874 | 0.05895 | -0.52769 |
| | R3 J s | 133.621 | 5532.070 | 0.02415 | 0.05895 | -0.60491 |
| | T b | 42.266 | 1019.440 | 0.04146 | 0.05895 | -0.30959 |
| | T s | 57.438 | 320.583 | 0.17917 | 0.05895 | 0.71299 |

The area of all landslides = 4174 Ha ,

The area of all catchment = 70793 Ha

Validation of the landslide susceptibility maps

The landslide susceptibility map derived from model was tested using the landslide data sets that were not used in model building process. For this, the total landslides observed in the study area were split into 2 parts, 145 (70 %) was randomly selected from the total 321 landslides as the training data and the remaining 63 (30 %) landslides are kept for validation propose. Spatial effectiveness of these susceptibility maps was checked by receiver operating characteristics (ROC). The ROC curve is a useful method for representing the quality of deterministic and probabilistic detection and forecast systems (Swets 1988). The area under the ROC curve (AUC)

characterizes the quality of a forecast system by describing the system's ability to predict correctly the occurrence or non-occurrence of predefined 'events'.

The model with higher AUC is considered to be the best. If the area under the ROC curve (AUC) is close to 1, the result of the test is excellent. On the other hand, if the model does not predict well, then this value will be close to 0.5. The prediction rate of the models was used for assessing the prediction capability of the models. The prediction rate explains how well the model and predictor variable predicts the landslide (Lee 2007). The prediction rate curve shows that the certainty factor model has high value of AUC (0.832) (fig.

3). From this, it is seen that the model employed in this study showed reasonably good accuracy in predicting the landslide susceptibility of the catchment.

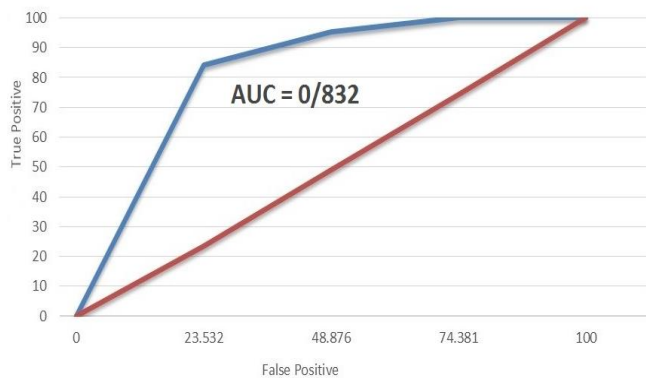


Fig 3. Rock curve for the landslide susceptibility maps produced by CF model.

Conclusions

Since landslides pose a serious threat to the life and property, their susceptibility mapping can be one of the preliminary steps toward minimizing the damages incurred by them. A landslide susceptibility map divides an area into various categories that range from stable to unstable ones. In this research certainty factor model was used for identifying the areas susceptible to land sliding in Latyan catchment, located in north Tehran, Iran. For this purpose, ten landslide conditioning factors (i.e., slope gradient; slope aspect; altitude; plan curvature; lithology; land use; distance from faults, rivers and roads; topographic wetness index (TWI) were used. A landslide inventory map was prepared using aerial photographs and extensive field survey. In this process, a total of 208 landslides were identified and mapped. Out of which, 145 (70 %) were randomly selected for generating a model and the remaining 63 (30 %) were used for validation purposes. The ROC plots showed that the susceptibility map produced using the model has the high prediction accuracy (83.20 %). This shows that the model employed in this study showed reasonably good accuracy in predicting the landslide susceptibility of Latyan catchment.

References

Akgun A, K incal C, Pradhan B (2011) Application of remote sensing data and GIS for landslide risk assessment as an environmental threat to Izmir city (west Turkey). *Environ Monit Assess.* doi: 10.1007/s10661-011-2352-8 (Article online first available)

Aleotti P, Chowdhury R (1999) Landslide hazard assessment: summary review and new perspectives. *Bull Eng Geol Environ* 58:21–44

Bednarik M, Magulova B, Matys M, Marschalko M (2010) Landslide susceptibility assessment of the Kralovany–Liptovsky Mikulas railway case study. *Phys Chem Earth Parts A/B/C* 35(3–5):162–171

Bednarik M, Yilmaz I, Marschalko M (2012) Landslide hazard and risk assessment: a case study from the Hlohovec–Sered' landslide area in south-west Slovakia. *Nat Hazards.* doi:10.1007/s11069-012-0257-7

Brabb EE (1984) Innovative approaches to landslide hazard mapping. In: *Proceedings 4th international symposium on landslides, Toronto, vol 1, pp 307–324*

Choi J, Oh HJ, Lee HJ, Lee C, Lee S (2012) Combining landslide susceptibility maps obtained from frequency ratio,

logistic regression, and artificial neural network models using ASTER images and GIS. *Eng Geol* 124:12–23

Chung CJ, Fabbri AG (1999) Probabilistic prediction models for landslide hazard mapping. *Photogramm Eng Rem S* 65(12):1389–1399

Constantin M, Bednarik M, Jurchescu MC, Vlaicu M (2011) Landslide susceptibility assessment using the bivariate statistical analysis and the index of entropy in the Sibiciu Basin (Romania). *Environ Earth Sci* 63:397–406

Guzzetti F, Reichenbach P, Cardinali M, Galli M, Ardizzone F (2005) Probabilistic landslide hazard assessment at the basin scale. *Geomorphology* 72:272–299

Jia N, Xie M, Mitani Y, Ikemi H, Djameluddin I (2010) A GIS-based spatial data processing system for slope monitoring. *Int Geoinf Res Dev J* 1(4)

Kanungo DP, Sarkar S, Sharma S (2011) Combining neural network with fuzzy, certainty factor and likelihood ratio concepts for spatial prediction of landslides. *Nat Hazards* 59:1491–1512

Karimi Nasab S, Ranjbar H, Akbar S (2010) Susceptibility assessment of the terrain for slope failure using remote sensing and GIS, a case study of Maskoon area, Iran. *Int Geoinf Res Dev J* 1(3)

Lee S, Min K (2001) Statistical analyses of landslide susceptibility at Yongin, Korea. *Environ Geol* 40:1095–1113

Lee S, Ryu JH, Won JS, Park HJ (2004) Determination and application of the weights for landslide susceptibility mapping: using an artificial neural network. *Eng Geol* 71:289–302

Magliulo P, Lisio AD, Russo F, Zelano A (2008) Geomorphology and landslide susceptibility assessment using GIS and bivariate statistics: a case study in southern Italy. *Nat Hazards* 47(3):411–435

Nefeslioglu HA, Gokceoglu C, Sonmez H (2008) An assessment on the use of logistic regression and artificial neural networks with different sampling strategies for the preparation of landslide susceptibility maps. *Eng Geol* 97(3–4):171–191

Oh HJ, Park NW, Lee SS, Lee S (2011) Extraction of landslide-related factors from ASTER imagery and its application to landslide susceptibility mapping. *Int J Remote Sens* 33(10):3211–323

Oh HJ, Pradhan B (2011) Application of a neuro-fuzzy model to landslide-susceptibility mapping for shallow landslides in a tropical hilly area. *Comput Geosci* 7(9):1264–1276. doi:10.1016/j.cageo.2010.10.012

Pourghasemi HR, Pradhan B, Gokceoglu C, Mohammadi M, Moradi HR (2012a) Application of weights-of-evidence and certainty factor models and their comparison in landslide susceptibility mapping at Haraz watershed, Iran. *Arab J Geosci.* doi:10.1007/s12517-012-0532-7

Pourghasemi HR, Pradhan B, Gokceoglu C, Deylami Moezzi K (2012b) A comparative assessment of prediction capabilities of Dempster-Shafer and Weights-of-evidence models in landslide susceptibility mapping using GIS, *Geomatics. Nat Hazards Risk.* doi:10.1080/19475705.2012.662915.

Pareek N, Sharma ML, Arora MK (2010) Impact of seismic factors on landslide susceptibility zonation: a case study in part of Indian Himalayas. *Landslides* 7(2):191–201

Pradhan B (2010a) Remote sensing and GIS-based landslide hazard analysis and cross-validation using multivariate logistic regression model on three test areas in Malaysia. *Adv Space Res* 45(10): 1244–1256.

- Pradhan B (2011a) Manifestation of an advanced fuzzy logic model coupled with geoinformation techniques coupled with geoinformation techniques for landslide susceptibility analysis. *Environ Ecol Stat* 18(3):471–493. doi: 10.1007/s10651-010-0147-7
- Pradhan B (2011b) Use of GIS-based fuzzy logic relations and its cross application to produce landslide susceptibility maps in three test areas in Malaysia. *Environ Earth Sci* 63(2):329–349
- Pradhan B, Chaudhari A, Adinarayana J, Buchroithner MF (2012) Soil erosion assessment and its correlation with landslide events using remote sensing data and GIS: a case study at Penang Island, Malaysia. *Environ Monit Assess* 184(2):715–727
- Pradhan B, Youssef AM (2010) Manifestation of remote sensing data and GIS on landslide hazard analysis using spatial-based statistical models. *Arab J Geosci* 3(3):319–326
- Pradhan B, Singh RP, Buchroithner MF (2006) Estimation of stress and its use in evaluation of landslide prone regions using remote sensing data. *Adv Space Res* 37:698–709
- Regmi NR, Giardino JR, Vitek JD (2010a) Modeling susceptibility to landslides using the weight of evidence approach: Western Colorado, USA. *Geomorphology* 115:172–187
- Saha AK, Gupta RP, Sarkar I, Arora KM, Csaplovics E (2005) An approach for GIS-based statistical landslide susceptibility zonation with a case study in the Himalayas. *Landslides* 2(1):61–69
- Swets JA (1988) Measuring the accuracy of diagnostic systems. *Science* 240:1285–1293.
- Van Westen CJ, Rengers N, Soeters R (2003) Use of geomorphological information in indirect landslide susceptibility assessment. *Nat Hazards* 30:399–419
- Varnes DJ (1984) Commission on landslides and other mass movements: landslide hazard zonation: a review of principles and practice. UNESCO Press, Paris 63 pp
- Wang HB, Wu SR, Shi JS, Li B (2011) Qualitative hazard and risk assessment of landslides: a practical framework for a case study in China. *Nat Hazards*. doi:10.1007/s11069-011-0008-1
- Xu C, Xu X, Lee YH, Tan X, Yu G, Dai F (2012) The 2010 Yushu earthquake triggered landslide hazard mapping using GIS and weight of evidence modeling. *Environ Earth Sci*. doi:10.1007/s12665012-1624.